

Are your **MRI contrast agents** cost-effective?

Learn more about generic **Gadolinium-Based Contrast Agents**.



**FRESENIUS
KABI**

caring for life

AJNR

Morphometric MRI Analysis: Improved Detection of Focal Cortical Dysplasia Using the MP2RAGE Sequence

T. Demerath, L. Rubensdörfer, R. Schwarzwald, A. Schulze-Bonhage, D.-M. Altenmüller, C. Kaller, T. Kober, H.-J. Huppertz and H. Urbach










This information is current as of April 19, 2024.

AJNR Am J Neuroradiol 2020, 41 (6) 1009-1014

doi: <https://doi.org/10.3174/ajnr.A6579>

<http://www.ajnr.org/content/41/6/1009>

Morphometric MRI Analysis: Improved Detection of Focal Cortical Dysplasia Using the MP2RAGE Sequence

 T. Demerath,  L. Rubensdörfer,  R. Schwarzwald,  A. Schulze-Bonhage,  D.-M. Altenmüller,  C. Kaller,  T. Kober,  H.-J. Huppertz, and  H. Urbach



ABSTRACT

BACKGROUND AND PURPOSE: Focal cortical dysplasias are the most common resected epileptogenic lesions in children and the third most common lesion in adults, but they are often subtle and frequently overlooked on MR imaging. The purpose of this study was to evaluate whether MP2RAGE-based morphometric MR imaging analysis is superior to MPRAGE-based analysis in the detection of focal cortical dysplasia.

MATERIALS AND METHODS: MPRAGE and MP2RAGE datasets were acquired in a consecutive series of 640 patients with epilepsy. Datasets were postprocessed using the Morphometric Analysis Program to generate morphometric z score maps such as junction, extension, and thickness images based on both MPRAGE and MP2RAGE images. Focal cortical dysplasia lesions were manually segmented in the junction images, and volumes and mean z scores of the lesions were measured.

RESULTS: Of 21 focal cortical dysplasias discovered, all were clearly visible on MP2RAGE junction images, whereas 2 were not visible on MPRAGE junction images. In all except 4 patients, the volume of the focal cortical dysplasia was larger and mean lesion z scores were higher on MP2RAGE junction images compared with the MPRAGE-based images ($P = .005$, $P = .013$).

CONCLUSIONS: In this study, MP2RAGE-based morphometric analysis created clearer output maps with larger lesion volumes and higher z scores than the MPRAGE-based analysis. This new approach may improve the detection of subtle, otherwise overlooked focal cortical dysplasia.

ABBREVIATIONS: FCD = focal cortical dysplasia; MAP = Morphometric Analysis Program

Focal cortical dysplasias (FCDs) are the most common epileptogenic lesions in children undergoing epilepsy surgery and the third most common cause in adults.¹ They encompass a broad spectrum of histopathologic abnormalities and have recently been classified in a 3-tiered system, in which FCD type I has abnormal radial and/or tangential laminations and FCD type II is composed of dysmorphic neurons either without (FCD IIa) or with (FCD IIb) balloon cells. FCD type III lesions

are dysplastic lesions occurring alongside other lesions, eg, hippocampal sclerosis or tumors.²

Whether a dysplastic lesion is detected on MR imaging depends on the degree of histopathologic abnormality and on the quality of the MR imaging examination.³ The impact of the MR imaging quality can be derived from the increasing proportions of FCD type II in cohorts of patients undergoing epilepsy surgery.⁴ Many of these FCDs were detected following postprocessing of an MPRAGE sequence, which highlighted subtle and thus equivocal findings on conventional, mostly FLAIR, sequences.^{5,6} For MR imaging postprocessing, several epilepsy centers use the Morphometric Analysis Program (MAP), which is based on algorithms of the freely available Statistical Parametric Mapping (SPM; <http://www.fil.ion.ucl.ac.uk/spm/software/spm12>) software. By comparison with a normal data base, 3 different morphometric maps are generated that highlight suspicious brain regions characterized by subtle blurring of the gray-white junction, abnormal cortical gyration, or abnormal cortical thickness.^{7,8}


The MP2RAGE sequence is a refinement of the MPRAGE sequence. It combines 2 MPRAGE datasets acquired, interleaved at different TIs, and creates a homogeneous T1-weighted contrast

Received January 23, 2020; accepted after revision March 24.

From the Departments of Neuroradiology (T.D., L.R., R.S., C.K., H.U.) and Epileptology (A.S.-B., D.-M.A.), Faculty of Medicine, Medical Center—University of Freiburg, Freiburg, Germany; Advanced Clinical Imaging Technology (T.K.), Siemens Healthcare AG, Lausanne, Switzerland; and Swiss Epilepsy Clinic (H.-J.H.), Klinik Lengg AG, Zurich, Switzerland.

Paper previously presented as a poster at: Annual Meeting of the German Society of Neuroradiology, October 3–6, 2018; Frankfurt, Germany.

Please address correspondence to Horst Urbach, MD, Department of Neuroradiology, University Medical Center Freiburg, Breisacher Str 64, 79106 Freiburg, Germany; e-mail: horst.urbach@uniklinik-freiburg.de

 Indicates article with supplemental on-line table.

<http://dx.doi.org/10.3174/ajnr.A6579>

Epilepsy-dedicated MR imaging protocol^a

MR Imaging Sequence	No. of Slices/Thickness (mm)	Voxel Size (mm ³)	T1/TR/TE/ α (ms/ms/ms/degree)	Acquisition Time (Min:Sec)
Sag 3D-MPRAGE	160/1	1 × 1 × 1	900/2000/2.26/12	4:40
Sag 3D-FLAIR-SPACE	160/1	1 × 1 × 1	1800/5000/388/var	6:52
Ax 2D-T2-TSE	42/3	0.4 × 0.4 × 3	5040/102/150	4:34
Ax 2D-T2*	23/5	0.7 × 0.7 × 5	639/19.9/20	2:33
Cor 2D-T2-STIR	40/2	0.4 × 0.4 × 2	100/5390/25/140	8:07
Cor 2D FLAIR	68/2	0.7 × 0.7 × 0.2	2500/9000/87/150	4:14
Ax 2D-DWI-SE EPI	23/5	0.6 × 0.6 × 5	3400/85	0:46
Sag 3D-MP2RAGE	192/1	1 × 1 × 1	700, 2200/2000/2.26/12	8:52

Note:—SPACE indicates sampling perfection with application-optimized contrasts by using flip angle evolution; SE, spin-echo; α , flip angle; Sag, sagittal; Ax, axial; Cor, coronal; var, variable flip angle.

^a 3T Magnetom Prisma (Siemens).

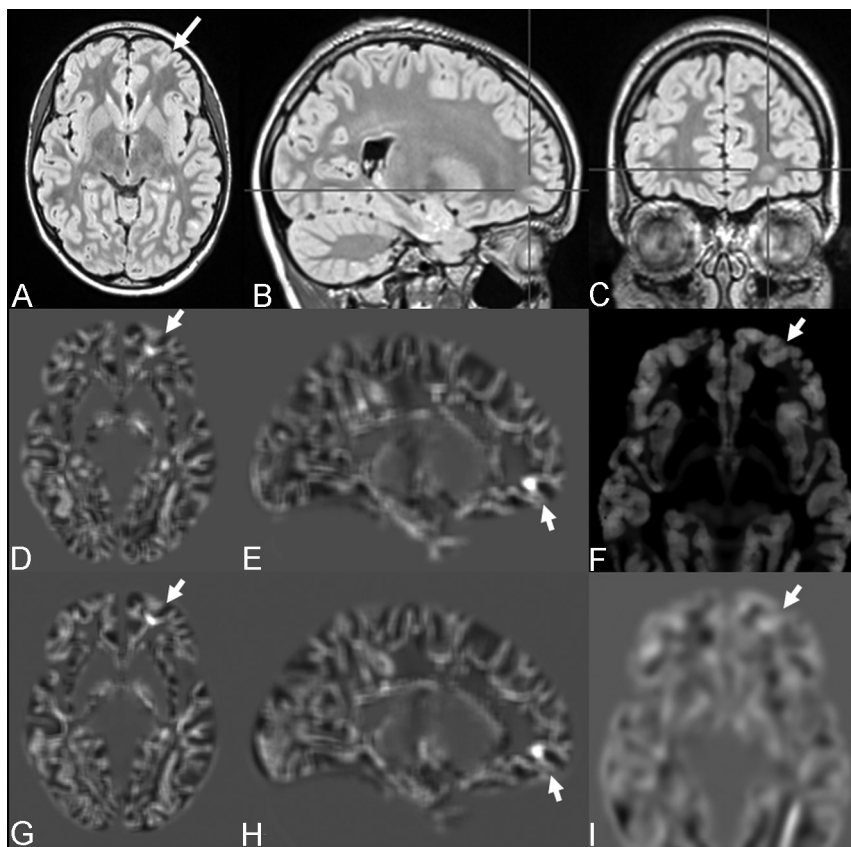


FIG 1. FCD with the transmantle sign of the left medial fronto-orbital gyrus (bottom-of-sulcus dysplasia) in a 12-year-old girl with seizures (patient 1). The lesion was overlooked on visual inspection (A–C) but was highlighted with MPRAGE-based (D and E) and MP2RAGE-based (G–H) junction images. MP2RAGE-based thickness (F) and extension (I) maps were considered to have negative findings.

with an intrinsic correction of B_1 inhomogeneities and reduced residual proton density and $T2^*$ weighting. $T1$ relaxation times can be derived from the MP2RAGE contrast, which has been shown to be highly reproducible both across subjects and within the same subject using different scanning parameters.⁹ We conducted this prospective study because we hypothesized that due to higher B_1 homogeneity, the MP2RAGE sequence is better suited for morphometric MR imaging analysis and the resulting FCD detection than the traditionally used MPRAGE sequence.

MATERIALS AND METHODS

Within a 4-year period (July 1, 2015–June 30, 2019), 640 patients with epilepsy were studied with an epilepsy-dedicated protocol¹⁰ and an additional MP2RAGE sequence on a 3T scanner (Magnetom Prisma; Siemens) (Table).

The study was in accordance with the 1964 Helsinki Declaration and its later amendments and was approved by the local ethics committee (University Medical Center Freiburg).

Morphometric MR Imaging Analysis

Morphometric MR imaging analysis was performed on MPRAGE and MP2RAGE images using a fully automated script, MAP, running in Matlab, Version R2014b (MathWorks). The current version of the program (MAP18) corresponds to previous implementations known as MAP07^{6,11,12} but now uses algorithms of SPM12, eg, the algorithm for normalization into Montreal Neurological Institute space known as “unified segmentation” (with small modifications in SPM12 compared with SPM5; see SPM12 Manual, page 51f, www.fil.ion.ucl.ac.uk) and the recently improved segmentation into 5 tissue classes instead of 3 as in SPM5. The creation of the morphometric maps has

been described in detail in previous publications.^{7,8,13,14} Briefly, each $T1$ input image is normalized to Montreal Neurological Institute space, simultaneously corrected for intensity inhomogeneities and segmented in different tissue compartments. The distribution of gray and white matter is analyzed on a voxelwise basis and compared with a normal data base. On the basis of this analysis, 3D morphometric maps, called extension image, junction image, and thickness image, are generated. These are z score maps in which brain regions that deviate from the normal data base have

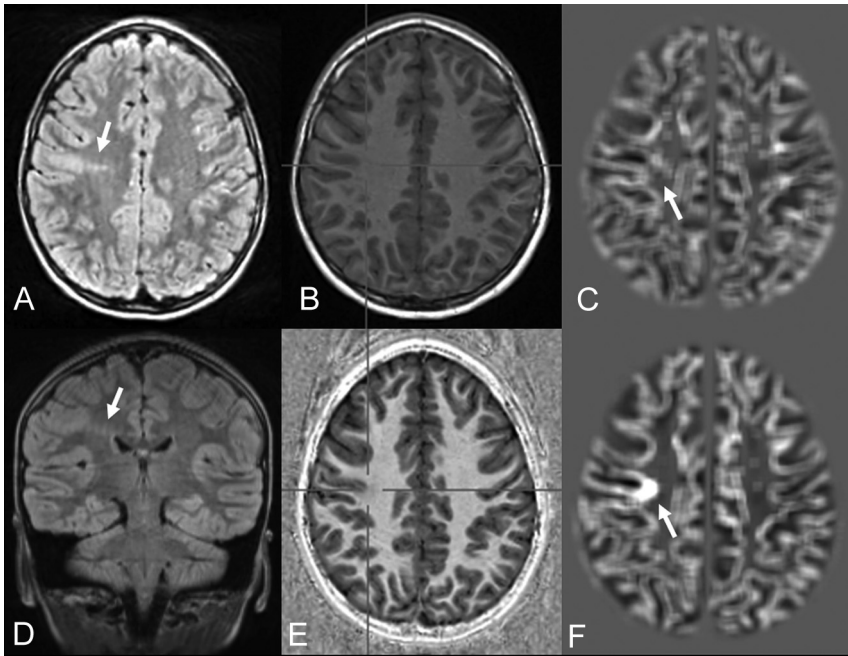


FIG 2. FCD with the transmantle sign of the right precentral gyrus in a 7-year-old girl with seizures (patient 18). Despite movement artifacts, the lesion is clearly visible on FLAIR (A and D) and MP2RAGE-based junction images (F). In an MPRAGE-based junction image (C) for comparison, the lesion is not clearly distinguishable. Strong T1WI contrast is seen in a uniform MP2RAGE image (E) compared with MPRAGE (B).

higher z scores and appear bright, thereby highlighting typical MR imaging features of FCDs, such as abnormal gyration and abnormal extension of gray matter into white matter (extension image), blurring of the gray-white matter junction (junction image), and abnormal cortical thickness (thickness image).

Because the junction image is the most sensitive of these maps, it was the focus of this study, and its creation will be described in more detail here:

Means and SDs of the voxel intensities in the gray and white matter compartments are used to determine individual lower (mean gray matter signal intensity + one-half gray matter SD) and upper (mean white matter signal intensity – one-half white matter SD) intensity thresholds for filtering and conversion of the normalized and intensity-corrected input image to a binary image. Each voxel with a gray value between these thresholds is set to 1 in the resulting binary image, and the other voxels are set to zero. The resulting binary image is then smoothed by a 3D convolution filter and compared with a normal data base. The datasets forming the normal database have been processed in the same way as described above and then used to create an average image and an image providing SDs for all voxel positions. These are used to transform the smoothed binary image into the final junction image with z score normalized data. Bright regions in the junction image correspond to cortical areas with a less defined border between gray and white matter and a broader transition zone compared with the normal data base.⁸

For the present study, 2 different normal data bases of healthy controls have been used, one for MPRAGE data and the other for MP2RAGE data. They consist of MPRAGE and MP2RAGE

datasets, respectively, of the same cohort of 154 persons (88 women, 66 men) with a mean age of 33.9 years (range, 20–64 years), measured on a 3T Magnetom Prisma scanner.

Evaluation

All morphometric maps (ie, junction, extension, and thickness images) were displayed in MRicro (<https://people.cas.sc.edu/rorden/mricro/mricro.html>) in the full-range contrast setting and screened alongside coregistered 3D-FLAIR sequences for dysplastic lesions. An FCD was diagnosed when the typical radiologic criteria were clearly identifiable on either T1 or FLAIR images. In such cases, lesions were manually segmented on axial slices of the junction images generated from MPRAGE and MP2RAGE sequences, respectively, according to the extent of the bright area highlighting the blurring of the gray-white matter junction. All segmentation results were stored as ROIs, and volumes and z scores were measured.

Thickness and extension images were evaluated only for positive or negative findings in a consensus reading by 2 readers with >3 and >20 years' experience in clinical neuroimaging. In this context, MPRAGE and MP2RAGE junction images were also examined for false-positive lesions, ie, findings without correlation in the FLAIR sequences.

Statistics

The Wilcoxon signed rank test was used to compare the volumes and z scores of the FCDs obtained with MPRAGE- versus MP2RAGE-based junction images. Statistical analysis and graphic representation were performed with SPSS 22 (IBM) and R (<https://www.R-project.org>).

RESULTS

Twenty-one lesions with MR imaging characteristics of FCD type II were identified in 20 patients (mean age, 27 ± 14.9 years; range, 7–60 years). An operation has been performed in only 7 patients so far (2 with FCD IIa, 4 with FCD IIb, and in 1 patient [patient 9] in whom only ectopic neurons were found). Seizure outcome has been available in 6 patients so far and was Engel Epilepsy Surgery Outcome Scale IA in 4 patients and IVB in 2 patients (patients 1 and 17; On-line Table).

Postprocessing of the MPRAGE and MP2RAGE sequences helped to detect 2 FCD IIa lesions, which were overlooked on conventional MR images (patients 1, 2; Fig 1). Two lesions (patients 14, 18; Fig 2) were invisible on MPRAGE-based junction images but clearly identified on MP2RAGE-based images. In 20 patients, we detected, in total, 34 (MPRAGE junction) and 32 (MP2RAGE junction) false-positive lesions, respectively (for individual values, see

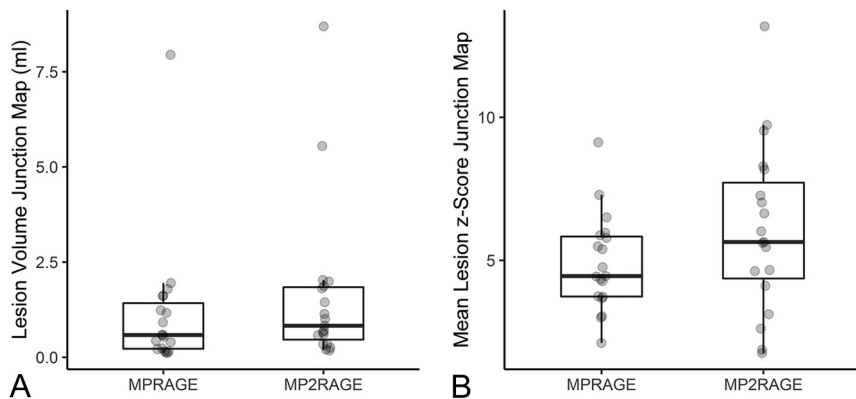


FIG 3. Lesion volumes (A, in milliliters) and mean lesion z scores (B) in MPRAGE- and MP2RAGE-based junction maps.

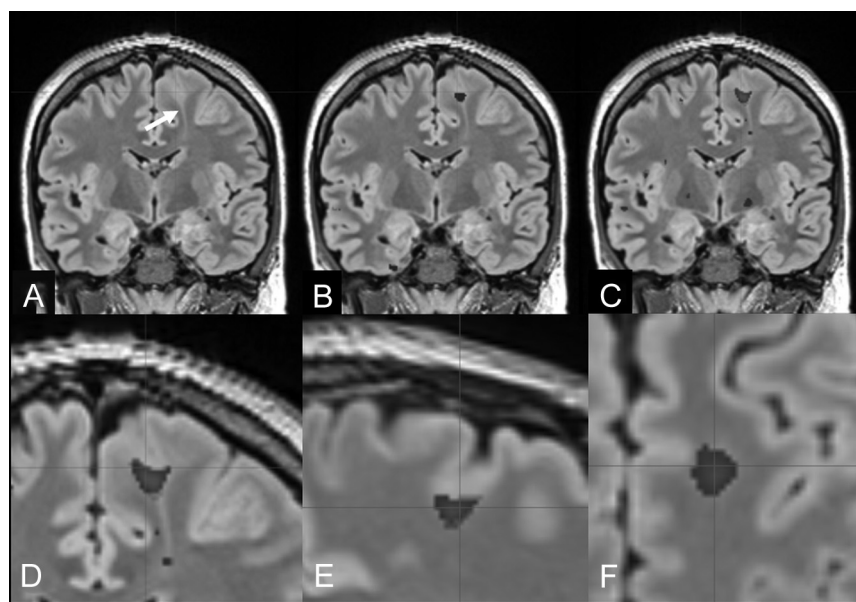


FIG 4. FCD IIb with a transmantle sign of the left superior frontal gyrus (bottom-of-sulcus dysplasia) in a 27-year-old man with right-sided sensory-motor seizures (patient 5). A, Reformatted 1-mm-thick coronal FLAIR section (*arrow*: transmantle sign of the FCD). B, Overlay of MPRAGE-based junction image abnormalities with z scores of >4 . C, Overlay of MP2RAGE-based junction image abnormalities with z scores of >4 . The MP2RAGE-based junction image matches the signal abnormalities at the gray matter junction as a characteristic feature of FCD type II (D–F, magnified coronal, sagittal, and axial views).

On-line Table). Distribution of false-positive findings was similar between both techniques, with no false-positives in 3 MPRAGE/6 MP2RAGE datasets, 1 false-positive in 7/6, two false-positives in 7/2, three in 1/4, four in 2/1, and 5 false-positive findings in 1 MP2RAGE dataset.

The median volumes of true-positive lesions, manually segmented on junction images, were 0.586 mL (range, 0.114–7.946 mL; standard error of the mean, 0.403 mL) for the MPRAGE-based junction images and 0.829 mL (range, 0.182–8.690 mL; standard error of the mean, 0.441 mL) for the MP2RAGE-based junction images, respectively ($P = .005$). The median z scores on full-range contrast junction images were 4.452 (range, 2.111–9.125; standard error of the mean, 0.381) for MPRAGE and

5.643 (range, 1.762–13.176; standard error of the mean, 0.654) for the MP2RAGE-based analysis, respectively ($P = .013$). The distribution of volumes and z scores, including median values, are presented in Fig 3.

A comparative analysis showed that MAP-junction was the most sensitive morphometric map (Figs 2, 4, and 5). Evidence of disturbed GM-WM differentiation was found in the MP2RAGE-based junction images of all 21 FCDs in 20 patients (On-line Table and Figs 1, 2, 4, and 5). In contrast, abnormalities in the thickness and extension images were only present in 13/21 and 16/21 lesions for the MPRAGE- and 13/21 and 18/21 lesions for the MP2RAGE-based analysis.

DISCUSSION

In the present study, postprocessing of an MP2RAGE sequence yielded larger lesion volumes and lesion z scores of the junction images compared with the MPRAGE sequence. In addition, it helped to detect 2 FCDs that were not highlighted on MPRAGE-based junction images.

The junction images display the abnormal transition of the gray-white matter junction. Blurring of the gray-white matter transition is a common feature in type I and II FCDs. The prevalence of transition zone abnormalities on structural (nonpostprocessed) MR imaging ranges between 53% (FCD Ia) and 79% (FCD IIb).¹⁵ The sensitivity and specificity of MAP junction maps in histology-proved FCDs, based on T1WI, have been reported as 64% and 96%.¹⁶

Displaying larger and brighter lesions, the MP2RAGE sequence likely

increases the sensitivity and diagnostic confidence, which may have an impact on the decision to proceed with invasive electroencephalography recordings or epilepsy surgery.

The abnormal cortical morphology as reflected by an increased cortical thickness and abnormal extension of gray matter into white matter is common in FCD II but is typically absent in FCD I and III. However, abnormal cortical morphology is more difficult to identify on the extension and thickness images than the abnormal transition of the gray-white matter junction on the corresponding junction images. In most cases, the lesions were detected with the aid of the junction images. However, there was a tendency for better detection of FCDs on MP2RAGE-based extension images (positive findings in 18/21 versus 16/21 lesions), whereas

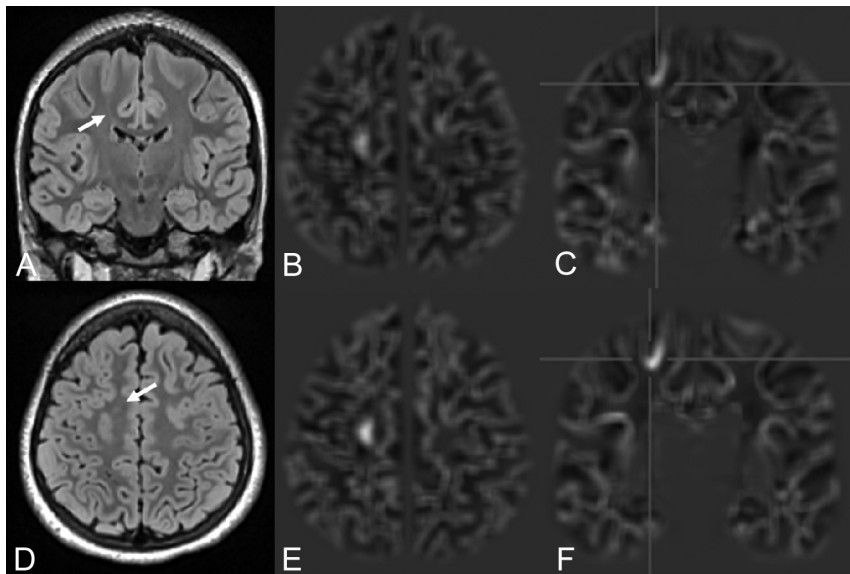


FIG 5. FCD with a transmantle sign of the right superior frontal gyrus (bottom-of-sulcus dysplasia) (FLAIR A and D) in an 11-year-old girl with left upper and lower limb somatosensory aura and motor seizures (patient 20). The MPRAGE- (B and C) and MP2RAGE-based junction images (E and F) match the signal abnormalities at the gray matter junction as a characteristic feature of FCD type II. MP2RAGE delivers, in this case, higher contrast junction images and better lesion definition compared with MPRAGE.

thickness images only had positive findings in 13/21 lesions in both techniques.

Our finding of larger lesion sizes in MP2RAGE-based MAP analysis raises the question about the real size of a lesion. By demonstrating larger lesion volumes, MP2RAGE-based junction maps may be superior in defining peripheral lesion components. Furthermore, positive findings on extension and thickness images suggest that an integrated definition and lesion detection in an automated approach represent the next step in MAP-based FCD postprocessing. Even if the resection of the subcortical component does not seem to improve the outcome, an integrative definition of the lesion component at the cortico-medullary junction should be sought.

Recently, a modification of the MP2RAGE sequence with altered TIs to null CSF and white matter in the 2 respectively acquired TI images has been published.¹⁷ The fluid and white matter suppression sequence appears ideally suited to search for FCD, but its use for morphometric analysis again requires the buildup of a sequence-specific normal data base of healthy controls.

A limitation of this study is the difficulty of evaluating whether in light of a higher sensitivity of MP2RAGE-based junction images, there are also more false-positive findings. In this study, we performed a qualitative visual evaluation with the aid of the results of the morphometric analysis. We did not use a specific threshold value for an automated detection of FCD, but re-assessed the “bright spots” on the morphometric analyses on FLAIR sequences to discover subtle lesions with abnormalities at the gray-white matter interface. Therefore, a further quantification and assessment of false-positive findings in patients or healthy controls is simply not possible. To at least estimate false-positive findings in patients, we visually compared MPRAGE- and MP2RAGE-based junction

images using the full-range contrast setting of MRICro. We found 34 and 32 false-positives in 20 patients on MPRAGE- and MP2RAGE-based images, respectively, with a similar distribution between both techniques. No differences with regard to the cluster size or the z scores of false-positives were found.

To estimate false-positive findings in healthy controls, we analyzed 70 healthy controls, assuming that they did not have FCD. With a general linear model and a leave-one-out strategy, each voxel was compared with the corresponding voxel of the remainder. Number and z scores of false-positive voxels ($P < .001$, $P < .05$ family-wise error-corrected) were not different between MPRAGE and MP2RAGE datasets (unpublished data).

However, at this point, for the detection of FCD in an epileptologic setting, sensitivity is more important than specificity or the number of false-positive findings because an undetected or overlooked lesion may prevent the patient from accessing an epilepsy surgery program.

Conversely, no putative FCD would undergo an operation directly, but first the epileptogenic potential of a possible lesion would always have to be verified using electrophysiologic methods. Therefore, a high sensitivity is more crucial for this type of clinical situation than a high specificity.

Another limitation is the relatively low number of FCDs and the fact that histopathologic proof has been obtained in only 7 patients so far. In 1 patient (patient 9), only ectopic neurons but no FCD were encountered. However, because the patient was seizure-free 3 months after the operation, a neuropathologic sampling error should also be taken into consideration.

Recently, a modification of the MP2RAGE sequence with inversion pulses to suppress CSF and white matter has been published.¹⁵ The fluid and white matter suppression sequence appears ideally suited to search for FCD but again requires the buildup of a data base of healthy controls and a larger number of patients with FCD.

CONCLUSIONS

MP2RAGE compared with MPRAGE produced junction images with larger FCD lesion volumes and higher lesion z scores, which may improve the detection of FCD in patients with focal epilepsy.

Disclosures: Andreas Schulze-Bonhage—UNRELATED: Board Membership: advisory boards on antiepileptic drugs of pharmaceutical companies; Consultancy: pharmaceutical and medical device consulting; Grants/Grants Pending: research on seizure detection and neurophysiologic correlates of cognition*; Payment for Lectures Including Service on Speakers Bureaus: lectures on epileptology. Tobias Kober—UNRELATED: Employment: Siemens Healthcare AG Switzerland,

Comments: full employment. Horst Urbach—UNRELATED: Board Membership: coeditor *Clinical Neuroradiology*; Payment for Lectures Including Service on Speakers Bureaus: Bayer AG, Stryker, UCB, Eisai Co, Bracco; OTHER RELATIONSHIPS: shareholder of VEObrain GmbH. *Money paid to the institution.

REFERENCES

1. Blumcke I, Spreafico R, Haaker G, et al; EEBB Consortium. **Histopathological findings in brain tissue obtained during epilepsy surgery.** *N Engl J Med* 2017;377:1648–56 [CrossRef Medline](#)
2. Blümcke I, Thom M, Aronica E, et al. **The clinicopathologic spectrum of focal cortical dysplasias: a consensus classification proposed by an ad hoc Task Force of the ILAE Diagnostic Methods Commission.** *Epilepsia* 2011;52:158–74 [CrossRef Medline](#)
3. Von Oertzen J, Urbach H, Jungbluth S, et al. **Standard magnetic resonance imaging is inadequate for patients with refractory focal epilepsy.** *J Neurol Neurosurg Psychiatry* 2002;73:643–47 [CrossRef Medline](#)
4. Bien CG, Raabe AL, Schramm J, et al. **Trends in presurgical evaluation and surgical treatment of epilepsy at one centre from 1988–2009.** *J Neurol Neurosurg Psychiatry* 2013;84:54–61 [CrossRef Medline](#)
5. Wagner J, Weber B, Urbach H, et al. **Morphometric MRI analysis improves detection of focal cortical dysplasia type II.** *Brain* 2011;134:2844–54 [CrossRef Medline](#)
6. Wang ZI, Jones SE, Jaisani Z, et al. **Voxel-based morphometric magnetic resonance imaging (MRI) postprocessing in MRI-negative epilepsies.** *Ann Neurol* 2015;77:1060–75 [CrossRef Medline](#)
7. Huppertz HJ, Grimm C, Fauser S, et al. **Enhanced visualization of blurred gray-white matter junctions in focal cortical dysplasia by voxel-based 3D MRI analysis.** *Epilepsy Res* 2005;67:35–50 [CrossRef Medline](#)
8. Huppertz HJ. **Morphometric MRI analysis.** In: Urbach H, ed. *MRI in Epilepsy*. Springer-Verlag; 2013:73–84
9. Marques JP, Kober T, Krueger G, et al. **MP2RAGE, a self bias-field corrected sequence for improved segmentation and T1-mapping at high field.** *Neuroimage* 2010;49:1271–81 [CrossRef Medline](#)
10. Urbach H, Mast H, Egger K, et al. **Presurgical MR imaging in epilepsy.** *Clin Neuroradiol* 2015;25(Suppl 2):151–55 [CrossRef Medline](#)
11. Wang S, Jin B, Aung T, et al. **Application of MRI post-processing in presurgical evaluation of non-lesional cingulate epilepsy.** *Front Neurol* 2018;9:1–7 [CrossRef Medline](#)
12. Wang W, Lin Y, Wang S, et al; Pediatric Imaging, Neurocognition and Genetics Study. **Voxel-based morphometric magnetic resonance imaging postprocessing in non-lesional pediatric epilepsy patients using pediatric normal databases.** *Eur J Neurol* 2019;26:969–71 [CrossRef Medline](#)
13. Kassubek J, Huppertz HJ, Spreer J, et al. **Detection and localization of focal cortical dysplasia by voxel-based 3-D MRI analysis.** *Epilepsia* 2002;43:596–602 [CrossRef Medline](#)
14. Huppertz HJ, Wellmer J, Staack AM, et al. **Voxel-based 3D MRI analysis helps to detect subtle forms of subcortical band heterotopia.** *Epilepsia* 2008;49:772–85 [CrossRef Medline](#)
15. Krsek P, Maton B, Korman B, et al. **Different features of histopathological subtypes of pediatric focal cortical dysplasia.** *Ann Neurol* 2008;63:758–69 [CrossRef Medline](#)
16. Wong-Kisiel LC, Tovar Quiroga DF, Kenney-Jung DL, et al. **Morphometric analysis on T1-weighted MRI complements visual MRI review in focal cortical dysplasia.** *Epilepsy Res* 2018;140:184–91 [CrossRef Medline](#)
17. Chen X, Qian T, Kober T, et al. **Gray-matter-specific MR imaging improves the detection of epileptogenic zones in focal cortical dysplasia: a new sequence called fluid and white matter suppression (FLAWS).** *Neuroimage Clin* 2018;20:388–97 [CrossRef Medline](#)